Review of in situ Test Methods for Solar Thermal Installations

Sven Fahr[1], Daniel Tschopp[2], Jan Erik Nielsen[3], Korbinian Kramer[1], Philip Ohnewein[2]

[1] Fraunhofer Institute for Solar Energy Systems ISE, Freiburg (Germany)

[2] AEE – Institute for Sustainable Technologies (AEE INTEC), Gleisdorf (Austria)

[3] PlanEnergi, Copenhagen (Denmark)

Abstract

The market for large solar thermal systems is growing and with it the need to plan, design and simulate these systems precisely. This requires the ability to accurately and meaningfully measure their performance and yields. Hence activities for the development of methods to characterize such plants are on-going. The paper presents three of these methods and compares them with regard to their technical requirements and boundary conditions. The comparison includes the collector models on which they are based, the nature of their results and the use cases for which they are most suitable. It should serve as a decision-making aid for stakeholders in selecting the measurement method best suited to their needs and boundaries. The paper shows that these methods do not contradict, but rather complement each other.

Keywords: Field measurement, collector certification, performance check, surveillance

1. Introduction

Large-scale solar thermal plants (>500 m² collector area, >350 kW_{th} nominal thermal power) are a cost-effective way to provide renewable heat (ESTIF, 2015). The market has experienced considerable growth recently, with close to 150,000 m² of solar collectors (105 MW_{th}) installed in large-scale systems in Europe in 2018 (Weiss and Spörk-Dür, 2019). The driving force has been solar district heating applications in Denmark, where the world's largest plant in Silkeborg (156,694 m² flat plate collectors; 110 MW_{th}) started operating in December 2016 (Weiss et al., 2017).

This market development has also drawn attention to the necessity of reliable and meaningful testing as the basis for energy yield simulation of such large-scale plants associated with large investments. At present, there are various activities for the development of such test procedures, which pursue different approaches and objectives. Three are selected here for discussion:

- An annex has been added to the Solar Keymark Scheme Rules to enable the measurement of collectors for product certification in the field based on results from the German funded project *ZeKon in-situ (In situ Collector Certification, ICC)*
- The Austrian funded research project *MeQuSo* developed methods for quality assessment of large-scale solar thermal plants under real operating conditions, based on similar physical foundations as the quasi-dynamic test method of ISO 9806 (ISO 9806, 2017) *(Dynamic Collector Array Test, D-CAT)*
- In ISO/TC 180 there is a new work item with a proposal for a simple method for checking collector field performance (ISO/AWI 24194, 2019) *(Performance Check for Collector Arrays, PC)*

Thus, there are different possible approaches in place potentially creating confusion as to which is the most preferable method for a specific application. This paper intends to provide clarity and transparency to manufacturers, plant designers and operators to be able to choose the suitable method providing them with the information needed within the acceptable cost and time frame.

2. Description of methodologies

2.1 In situ collector certification (ICC)

Introduction

Within the scope of the project *ZeKon in-situ* funded by the German Ministry of Economic Affairs and Energy, research was carried out into how a single collector in a field installation can be characterized for certification purposes on the basis of an adapted quasi-dynamic test method (QDT) known from ISO 9806 (ISO 9806, 2017). The necessary adaptations of the test method and a new Appendix P5.5 to the Solar Keymark Scheme Rules were developed, which describes the procedure and peculiarities of field measurements on the level of product certification. The flowchart in Fig. 1 shows the process of the method.

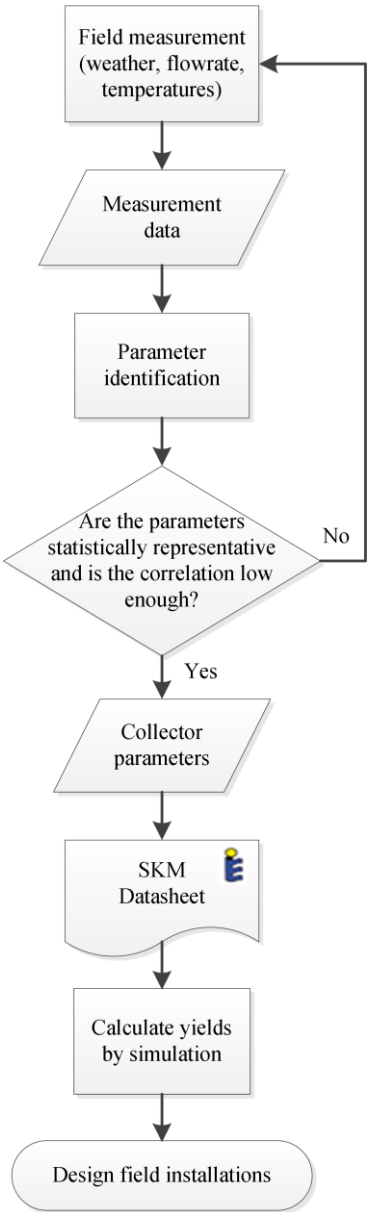

Fig. 1: Process diagram of a field certification measurement

Scope and use case

"In-situ certification is targeting but not limited to collectors which because of their size, power output, weight, operating conditions or on-site production can hardly be tested in a laboratory" (SKN Working Group, 2019). The method can therefore be applied to any collector type. The information and results that can be generated with such a measurement are the same as for a certification test in the laboratory. The aim of such a measurement is always a parametrization of the collector, usually for the purpose of obtaining a Solar Keymark certificate. On the basis of the specific parameters, systems can be designed and expected collector yields calculated and compared.

In addition to the above-mentioned reasons for field measurements, the method was also developed against the background that the collector parameters based on laboratory measurements were partly criticized as being not representative in the past. Each manufacturer is now free to have his product tested either in the laboratory or in a field installation, which is, however, associated with increased effort.

Methodology

The collector is measured according to the collector model standardized in ISO 9806 and as far as possible also using the QDT method described there.

In comparison to laboratory measurement, differences in the procedure arise mainly in the following points:

- Boundary conditions of the measurement:

In order to enable the collector to be measured in regular system operation without interfering with the control system, the boundary conditions specified in the standard, in particular the permissible fluctuation of input temperature and mass flow rate as well as the averaging time span used, must usually be adapted. Their influence was investigated in a sensitivity analysis within the framework of the project. Averaging times of 5 minutes worked out for the best results. Very short averaging times or instantaneous data are hardly suitable for this method. With sufficiently long averaging times, fluctuation limits of up to 5K in the input temperature and up to 15% in the mass flow could be allowed and led to good results (Fahr et al., 2018).

All sequences with potential shadowing are excluded from the measurement based on geometrical calculations.

- Measurement technology:

Deviating from the standard, a SPN1 sensor can be used to measure the diffuse radiation. This comes with the

advantage that neither manual adjustment nor a tracking device is needed, hence significantly reducing the maintenance effort and costs. The use of this sensor for global radiation measurement also showed good results in the project with minor deviations compared to standard measurement technology, but is not yet permissible. The use of non-invasive flow rate measurement technology is generally not prohibited by the standard if the corresponding measurement uncertainty is adhered to. However, the project showed that this is only possible under very specific flow conditions and that the application is difficult in most cases. As expected, the use of surface temperature sensors led to large deviations and is therefore not recommended.

Results

In the project *ZeKon in-situ* it was shown that it is possible to generate parameters for collectors in the field. Slight deviations from the laboratory measurement are within confidence interval of the reference measurement. This was achieved by using the measurement equipment described above and extended limits for the permissible boundary conditions. In Fig. 2 a comparative measurement is shown for an exemplary collector.

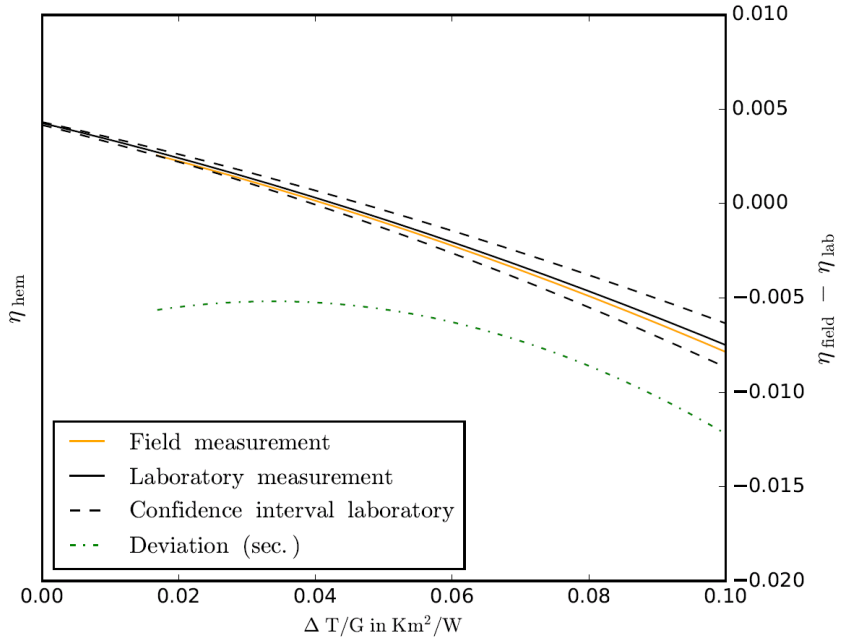

Fig. 2: Measurement results from laboratory and field for an exemplary collector of identical design

A sufficient variance of the measured values with regard to all parameters to be determined is indispensable and not always easy to achieve in the field. This applies in particular to the collector input temperature and, in the case of biaxial collectors, the angle of incidence of both axes. The acquisition and combination of measurement data from more than one collector of a row (at least the very first and last, more if necessary) can be helpful in order to obtain data at different temperature levels. An extrapolation of the efficiency curve is only permissible in the range described by the standard, as applied in Fig. 2. It is advisable to precisely analyze the feasible boundary conditions in advance of such a measurement campaign.

Of great importance in such a measurement is the assessment of the parameter quality, which depends to a large extent on the quality of the underlying measurement data. A detailed evaluation of the parameter quality is possible, for example, with the so-called bootstrapping procedure. This involves imposing artificial noise on the data set on the basis of the residuals between the power measured and the power calculated during parameterization. The residuals of randomly selected measurement sequences from the original data are used to generate a large number of new data sets, which can then be parameterized again. This process is repeated many times and thus a large number of different parameter sets for the collector are generated, whose distribution and co-variances can then be analyzed and used to assess the quality of the parameters (Zirkel-Hofer et al., 2018). Significant dependencies between different parameters as well as distributions of individual parameters, which deviate strongly from a normal distribution, can indicate an insufficient database. The confidence intervals of the individual parameters also serve as indication for the quality of the evaluation. Tools for the automated application of bootstrapping on the evaluated data have been developed at Fraunhofer ISE and applied within *ZeKon in-situ*.

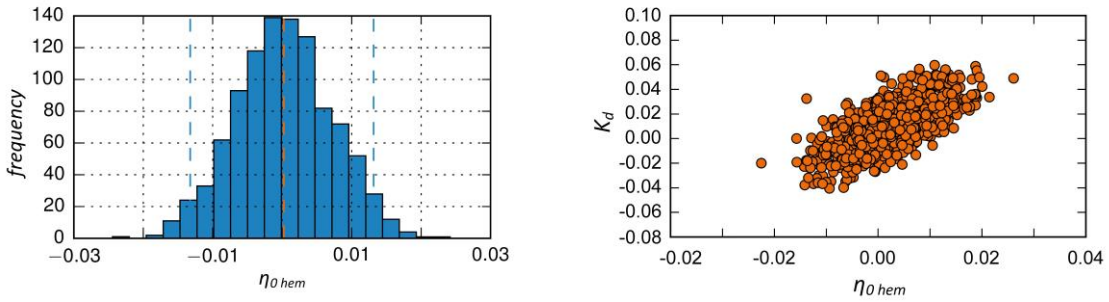

Fig. 3: Exemplary graphs for parameter distribution (left) and covariance (right) from bootstrapping

Fig. 3 shows two exemplary graphs resulting from bootstrapping to demonstrate how it helps to assess the parameter quality. On the left side the distribution of $\eta_{0,hem}$ (normalized to the originally determined parameter value) for an exemplary field measurement is presented. The dotted orange line marks the median value and the blue dotted lines represent the 95% confidence interval. In this case the confidence interval of the conversion factor ($\eta_{0,hem}$) is close to what is typical for a laboratory measurement. In combination with the nearly normal distribution it indicates that the underlying data basis allows a meaningful non-biased determination of the parameter.

On the right side of Fig. 3 an example for the covariance between $\eta_{0,hem}$ and K_d is shown (normalized to the originally determined parameter values). It indicates a clear correlation of high values for $\eta_{0,hem}$ with high values for K_d, meaning that on basis of the underlying data set both parameters could not be identified completely independent. The strength of a correlation can be measured by the correlation coefficient, which can range from 0 (fully independent) to 1 (fully dependent) and is 0.7 in this example. A result like this implies the requirement for further assessment of sufficient variability in the measurement data. This mathematical data point evaluation is most helpful to have un-biased collector parameters for different products from field measurement, without the need of a new model.

2.2 Dynamic Collector Array Test (D-CAT)

Introduction

The Dynamic Collector Array Test (D-CAT) is an in situ test method for quality assessment of large collector arrays under fully dynamic operating conditions. The method has a similar physical modeling approach for single collectors as the quasi-dynamic test procedure of ISO 9806, but extends the ISO model to collector rows and collector arrays. The method has been developed in the Austrian funded research project *MeQuSo*. It is currently in a proof of concept state. The description below gives the present status, minor changes are possible.

Scope and use case

The D-CAT method uses a parameterized collector array model which is applicable to typical array configurations of large-scale solar thermal plants. In the current state of development, the D-CAT method is limited to arrays with flat plate collectors, although extensions to other collector types are possible within the existing framework.

The main goal of the method is to obtain a set of parameters of this model to characterize the behavior of the collectors based on measured operating data. The model accepts fully dynamic inputs and can thus be applied to fully dynamic conditions of the normal plant operation. That is, the method does not require running special test sequences or pre-filtering data to obtain "quasi-dynamic" states. A central feature of the D-CAT method is the fact that it can be run in automated mode and therefore repeated in time with little additional effort.

Performance reductions that concern the collectors on a component level (such as soiling, broken insulation, faulty foil tension etc.) are reflected in the estimated parameters to obtain a characterization of the collectors under 'real-world' conditions (Tschopp et al., 2017). Heavily soiled collectors will have worse values for the optical parameters than clean collectors. On the contrary, performance relevant factors which do not accrue from the collector on a component level (such as local weather conditions, operating conditions, collector array

geometry, hydraulic setup, etc.) are not mirrored in the estimated parameters. A collector array operated at higher temperatures will have a lower efficiency, but the same collector parameters as an array operated at lower temperatures.

The in situ parameterization of a collector array can be used as follows:

- commissioning: target/actual comparison with guaranteed thermal power output/yield
- surveillance: detecting trends with repeated testing
- control: parametrization of collector array models
- testing at different locations: transparent comparison of collector arrays

Methodology

The flowchart in Fig. 4 below shows the process of the method.

Performance boundaries

The performance boundary is the collector array including the collectors and connection pipes between the collectors (Fig. 8). Not included are the distribution pipes from the array to the heat exchanger.

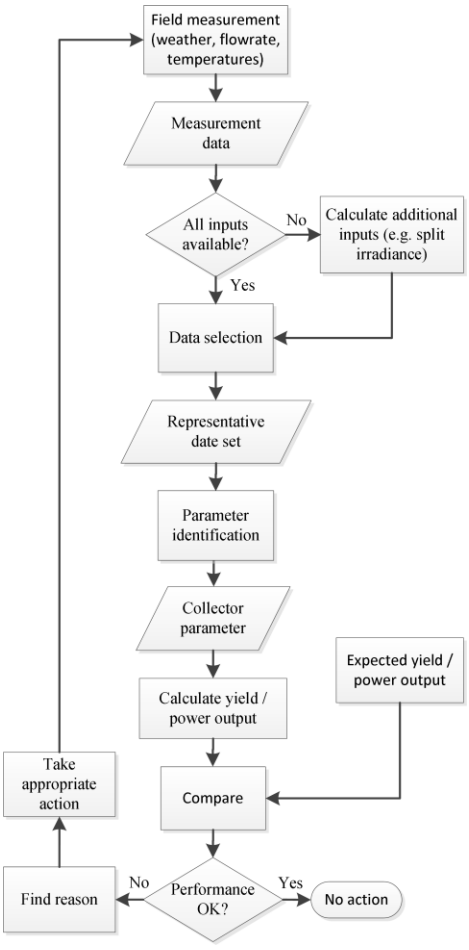

Fig. 4: Flowchart for processing the Dynamic Collector Array Test (D-CAT) method

Modeling

A one-node model (fluid temperature node) and two-node model (fluid and solid temperature nodes) can be used. Both models take into account that collector rows are relatively long in large arrays, so the temperature is assumed to change depending on the position along the fluid direction. The partial differential equations (PDE) for a specific position are given below:

One-node model:

$$\dot{m}_{pri}\, c_{f,x} \frac{\partial \vartheta_{f,x}}{\partial x} = \eta_{0,b}\, K_b(\theta) \cdot s \cdot G_b + \eta_{0,b}\, K_d\, G_{d,avg}$$

$$-a_1\left(\vartheta_{f,x} - \vartheta_a\right) - a_2\left(\vartheta_{f,x} - \vartheta_a\right)^2 - a_5\left(\frac{\partial \vartheta_{f,x}}{\partial t}\right) \qquad \text{(eq. 1)}$$

Two-node model:

$$\dot{m}_{pri}\, c_{f,x} \frac{\partial \vartheta_{f,x}}{\partial x} = b_0\left(\vartheta_{s,x} - \vartheta_{f,x}\right) - c_{f\_A,x}\left(\frac{\partial \vartheta_{f,x}}{\partial t}\right) \qquad \text{(eq. 2a)}$$

$$b_0\left(\vartheta_{s,x} - \vartheta_{f,x}\right) = (\tau\alpha)\, K_b(\theta) \cdot s \cdot G_b + (\tau\alpha)\, K_d\, G_{d,avg}$$

$$- b_1\left(\vartheta_{s,x} - \vartheta_a\right) - b_2\left(\vartheta_{s,x} - \vartheta_a\right)^2 - b_5\left(\frac{\partial \vartheta_{s,x}}{\partial t}\right) \qquad \text{(eq. 2b)}$$

The modeling has the following distinct features:

- The explained variable of the model equations is not the thermal power output like in ISO 9806, but the measured outlet temperature and additional temperatures within the collector array which are not measured (grey-box model).
- Fluid propagation (transport) is modelled in the spatial derivative terms. While this increases the model complexity, it is a crucial feature especially for estimating the collectors' heat capacity because travel times of the fluid through the array is oftentimes comparable to the collectors' time constant (Lemos et al., 2014).
- For collectors within an array, sky and ground view are obstructed due to collectors placed in front (Appelbaum, 2018). This reduces the diffuse irradiance along the collector height from top to bottom. The D-CAT method calculates an average diffuse irradiance which corrects for this effect. For

laboratory tests, there is no view obstruction, and a correction of the measured irradiance at the top of the collector is not necessary.

- Contrary to ISO 9806, wind heat losses are not included in the model, as the wind speed above the collector cannot be representatively measured for collector arrays. For collectors with high wind heat losses, data with high wind speed should be discarded.
- Operating conditions with internal shading can be included if the share of the collector array which is shaded can be determined with reasonable accuracy and the shading share is low.
- The two-node model is typically substantially superior in explaining dynamic behavior, but it lacks direct comparability with the quasi-dynamic ISO 9806 parameters. It is recommended to use the two-node model when the residuals of the transient collector array operating conditions are large.

The model equations have no analytical solution. They are solved numerically based on the method of lines: The temperatures are discretized in flow direction based on a one-dimensional finite volume method (LeVeque, 2002). This results in a system of ODEs which can be efficiently solved by appropriate stiff ODE solvers. This approach calculates all heat transfers based on the local temperature of each finite volume segment. For (eq. 1) this leads to the same collector parameters as in the ISO 9806 equation.

Measurement setup and data acquisition

Since D-CAT is a method taking into account fully dynamic behavior, it requires relatively high sampling rates of not more than 1 minute and ideally 10 seconds or less. The required inputs that are used for the parameter estimation are the mass flow rate of the collector array, the return and flow temperature at the entry and exit points to the collector array, the total irradiance in the collector plane (or any other surface) and the heat capacity of the fluid. The method contains an advanced radiation processing algorithm which splits the total radiation in its direct and diffuse part (if only the hemispherical radiation is measured). Other measurement setups are possible. In these cases, a simulation procedure is used to calculate the model inputs at the performance boundaries.

Data processing and performance assessment

A key part of the D-CAT method is the data selection, which is done in three steps:

1. Only include data where the model is applicable. All operating conditions above a minimal thermal power output level, below an internal shading share threshold and conditions where no external shading occurs can be used. Variable volume flows and rapid return temperature changes (typical when using speed-controlled pumps) are acceptable.
2. Intervals with 90 minutes of continuous operation are retrieved/selected.
3. Typically, some type of intervals (e.g. intervals with high irradiance and constant operation temperatures during the summer months) are overrepresented, which can lead to overfitting and high correlation of the parameters. To address this problem, a subset of (typically around 25) optimal intervals is selected automatically, where each interval makes a substantial contribution to determine the model parameters. This can be interpreted as an optimal design problem, where the total interval information is maximized by maximizing the determinant of the Fisher information matrix (D-optimality criterion) (Federov, 2013).

Based on the retrieved intervals, the parameter estimation is done by minimizing a cost function, the RMSE of the deviation between measured and simulated array outlet temperatures. The simulation of an interval requires knowing the initial conditions (the temperatures of the finite volume segments) which are not measured. To overcome this problem, the first 30 minutes of an interval are used for a pre-simulation to get a good assumption of the initial conditions for the simulation of the main 60-minutes-intervals. The aim is to include measurement and modeling uncertainty in the parameter estimation in the next development step of the method.

Results

The D-CAT method allows an in situ parameterization of the collectors in the collector array (such as zero loss efficiency, heat loss coefficients, thermal capacity, etc.). Fig. 5 shows typical results for the efficiency and

incidence angle modifier curves when a collector array is tested at inauguration and after multiple years of operation. For each test run, different parameter values ("in situ parameters") are obtained which mirror the current state of the collectors. For this collector array, the performance of the collectors at inauguration is a bit below the datasheet. The performance is further reduced after multiple years of operation (possibly due to soiling). A thermal power output guarantee can be checked by comparing the thermal power output/efficiency based on datasheet parameters versus in-situ parameters for defined operating conditions. A yield guarantee can be checked by comparing the simulated solar yield with the data sheet parameters versus in-situ parameters.

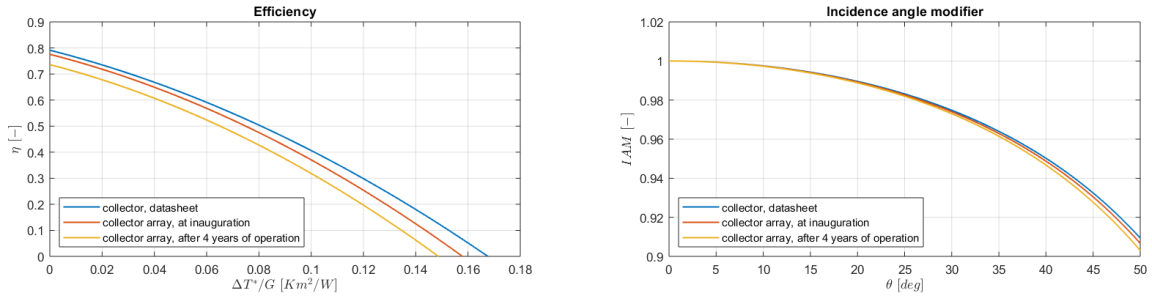

Fig. 5: Efficiency and incidence angle modifier curves with datasheet versus in situ parameters

2.3. Performance Check for Collector Arrays (PC) - ISO/TC 180 work item

Introduction

This Performance Check (PC) method - or similar - has been used in Denmark for approx. 10 years to check performance of large-scale solar collector fields for district heating. It was described in fact sheets in IEA SHC Task 45 (Nielsen 2014a, 2014b). It has now been proposed as an input to a new ISO standard, and a working group under ISO/TC180 is elaborating this standard right now. The description below gives present status, the final standard may derive.

Scope and use case

This method can be used for a simple check of the collector field power performance. It can be used in connection with the commissioning of the collection field and/or for continuous on-line surveillance. It can be used for flat plate collectors and for concentrating collectors.

Methodology

The overall principle is to check the measured power against the estimated power when the collector field is running close to full power.

Calculating estimated power

The estimated power is calculated based on collector parameters from ISO 9806 testing plus some safety factors. The equation used for estimating the collector field power is chosen depending on collector type and the wanted uncertainty level. Three equations are available:

Equation A: A simple power performance estimate for non-concentrating collectors:

$$\dot{Q}_{sec,est} = n_{col} \cdot A_G \cdot [\eta_{0,hem} G_{hem} - a_1 (\vartheta_{m,cf} - \vartheta_a) - a_2 (\vartheta_{m,cf} - \vartheta_a)^2 - a_5 (d\vartheta_{m,cf}/dt)] \cdot f_{safe} \quad \text{(eq. 3)}$$

Equation B: A more advanced equation for non- or low-concentrating collectors (concentration ratio $C_R < 20$) can be used if the direct and diffuse radiation on the collector plane is available. Using eq. B will normally give results with smaller uncertainty than using eq. A as incidence angle modifiers for the collector are considered in eq. B.:

$$\dot{Q}_{sec,est} = n_{col} \cdot A_G \cdot [\eta_{0,b} K_b(\theta_L, \theta_T) G_b + \eta_{0,b} K_d G_d - a_1 (\vartheta_{m,cf} - \vartheta_a) - a_2 (\vartheta_{cf,m} - \vartheta_a)^2 - a_5 (d\vartheta_{m,cf}/dt)] \cdot f_{safe} \quad \text{(eq. 4)}$$

Equation C: Is used for concentrating collectors with high concentration ratio $C_R \geq 20$ – tracking in one or two axis and utilizing mainly or only the direct radiation.

$$\dot{Q}_{sec,est} = n_{col} \cdot A_G \cdot [\eta_{0,b} K_b(\theta_L, \theta_T) G_b - a_1 (\vartheta_{m,cf} - \vartheta_a) - a_5 (d\vartheta_{m,cf}/dt) - a_8 (\vartheta_{m,cf} - \vartheta_a)^4] \cdot f_{safe} \quad \text{(eq. 5)}$$

f_{safe} is taking into account pipe and other heat losses, measurement uncertainty and other uncertainties.

To limit uncertainties, some restrictions on the operations conditions are given: No shadows; moderate change in collector mean temperature; no risk of snow/icing; no high wind – and if eq. A is used: incidence angle < 30°. Only measurement points which satisfy these restrictions are valid.

Power measurement

Although the performance is checked for the primary loop, it's recommended to measure the power output on the secondary side to avoid uncertainties due to the physical values of the collector loop fluid. So, collector field power $\dot{Q}_{sec}$ shall be measured on the secondary side of the heat exchanger, based on flow and temperature measurements:

$$\dot{Q}_{sec} = \dot{V}_{i,sec} \cdot \rho_{i,sec} \cdot c_{f,sec} \cdot (\vartheta_{e,sec} - \vartheta_{i,sec}) \quad \text{(eq. 6)}$$

The flowchart in Fig. 6 below shows the process of the method.

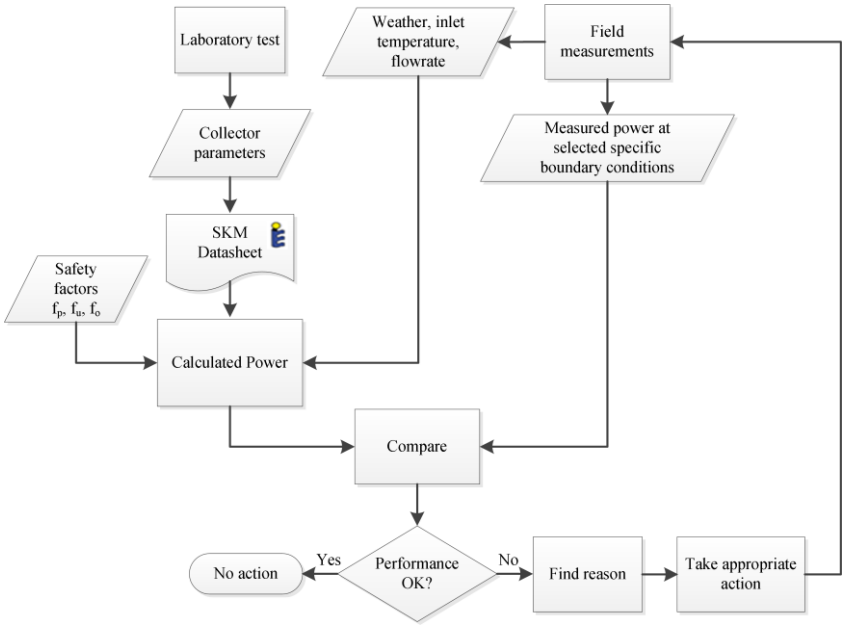

Fig. 6: Flowchart for processing the Performance Check (PC) method

Measurement equipment

The necessary measurement equipment for measuring the collector field power output is indicated in Fig. 8 below.

The equipment for solar irradiance measurement follows from the equation used:

- Eq. A: Global irradiance measurement in the collector plane is needed.
- Eq. B: Direct and diffuse irradiance measurement is needed, options are:
  - Pyranometer for global irradiance in the collector plane + pyranometer with shadow ring for diffuse irradiance in the collector plane
  - Pyranometer for global irradiance in collector plane + pyrheliometer for beam irradiance
- Eq. C: Only pyrheliometer for beam irradiance is needed.

Other equipment:

- Energy meter (flow meter + temperature sensors in secondary (water) loop)
- Temperature sensors for in- and outlet of heat exchanger primary loop
- Temperature sensor for ambient air temperature
- Anemometer for wind velocity

Logging / recording:

Measurement data are logged (and calculated) at least each minute. Averaged data are recorded (at least) each hour.

Uncertainty levels:

Present version of the method has two levels of uncertainty – first level one corresponds more less to the ISO 9806 uncertainty level – second level is more relaxed.

Results

The main final result is the deviation between summarized estimated and summarized measured performance given as a percentage:

Deviation in $\dot{Q}$:

$$d\dot{Q}_{\%} = (\dot{Q}_{sec} - \dot{Q}_{sec,est}) / \dot{Q}_{sec} \qquad \text{(eq. 7)}$$

Supplementary results are presented in Fig. 7, showing the measured data points for power output against the corresponding estimated power on the left side and the average measured and estimated power on the right.

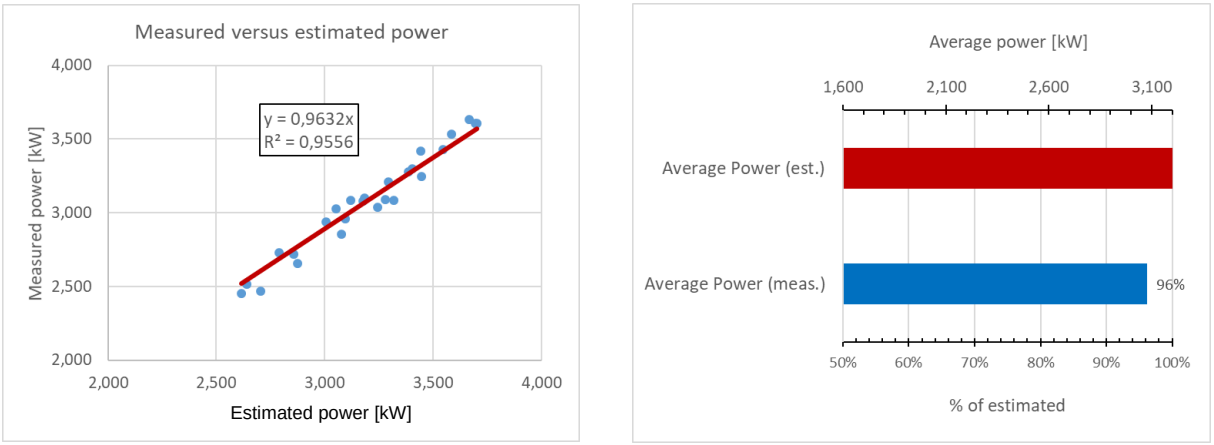

Fig. 7: Measured points of power versus estimated points of power (left) and average measured power versus average estimated power (right)

3. Comparison of the methodological approaches

3.1 Measurement setups

The system layout with sensor locations and performance measurement boundaries for all three methodological approaches is shown in Fig. 8.

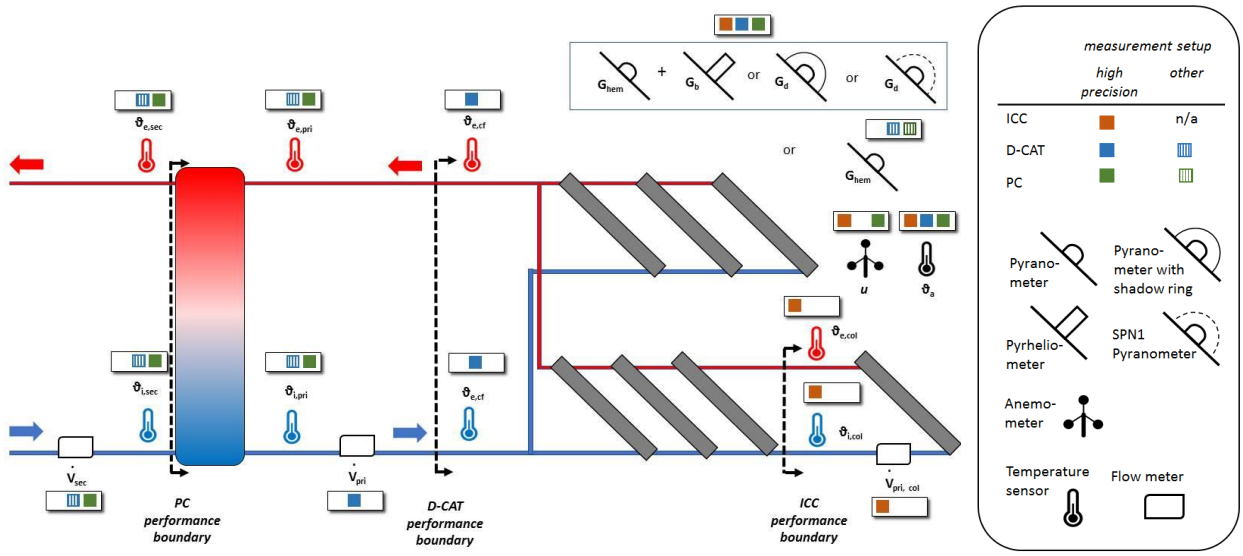

Fig. 8: System layout, sensor locations and performance boundaries

While the ICC method generates collector parameters from measurement data taken directly at (one or more) single collectors, the D-CAT method takes measurement data from the complete collector field (excluding distribution pipes) and uses a collector field model with correction terms for different factors influencing the field to derive collector parameters. The PC method refers to the complete field including the distribution pipes and recommends measuring the power output in the secondary loop.

3.2 Distinguishing features

To give an overview of the differences between the described methods, their distinctive properties are summarized in Tab. 1.

Tab. 1: Distinctive properties of the test methods

Test procedure	**ISO 9806** Laboratory testing	**ICC** In situ collector certification	**D-CAT** Dynamic Collector Array Test	**PC** Performance Check for Collector Arrays
Basics				
Use case (main)	collector certification	collector certification, evaluating single collectors in field installation	performance check and surveillance based on in situ collector array parametrization under fully dynamic conditions	performance check under stable conditions close to full power operation, surveillance
Test site	laboratory	In situ	In situ	In situ
Test object (performance measurement boundaries)	single collector	single collector(s)	collector array without pipes	collector array including pipes and heat exchanger
Collector types	all	all	flat plate; extensions to other collector types possible	all
Status	standard	permissible; Annex P5.5 of Solar	proof of concept completed	input to standardization work

		Keymark Scheme Rules		item in ISO TC 180
Test outcome				
Key performance indicators	normative collector parameters	normative collector parameters	collector parameters describing the measured behaviour of the collectors in the array	target/actual comparison based on ISO 9806 data sheet parameters
Solar yield estimation	✓	✓	✓	×
Model				
Explained variable	thermal power output	thermal power output	outlet temperature	thermal power output
Collector model	steady state, quasi-dynamic	quasi-dynamic (ISO 9806)	dynamic model calculated into ISO 9806 parameters; additional 2-node model	three equations based on collector types (used for target performance comparison, but not parameter estimation)
Additional collector array modelling	-	-	effective direct and diffuse radiation, distribution pipes, heat exchanger (depending on sensors)	reduction factors for distribution pipes and heat exchanger losses
Measurement setup, data procession				
Required sensors	standard high precision sensors	standard high precision sensors, alternative sensors for diffuse irradiance measurement allowed	irradiance, air temperature, fluid temperatures, volume flow; low precision sensors possible	irradiance, air temperature, wind velocity, fluid temperatures, volume flow
Duration of measurement	4-5 days	minimum 5-10 days, up to 6 months (depending on collector type and operation conditions)	minimum 4-5 days, up to 6 months (depending on operation conditions)	minimum 4-5 days, up to 6 months (depending on operation conditions)
Test data	defined test sequence	normal plant operation	normal plant operation	normal plant operation
Main boundary conditions	strict limits especially regarding inlet temperature and mass flow rate stability; no shading, no high wind	extended limits for inlet temperature and mass flow rate stability; no shading, no high wind	no external shading; internal shading allowed in some circum-stances; minimum 90 minutes of continuous operation	no shadows; moderate change in collector mean temperature; no risk of snow/icing; no high wind – and if eq. 1 is used: incidence angle < 30^0

Sampling rate / Averaging time	< 10s / no specifications	< 10s / multiple times the pass-through time of fluid through collector recommended	≤ 1 min / 10s for data with sampling rate < 10s, otherwise not necessary	≤ 1 min / 15 – 60 min
Requirements for data handling	spread sheet	spread sheet, additional software tools for automated plausibility checks and analysis of parameter quality recommended	programming skills required (e.g. Python, R, MATLAB®), but test can be completely automated	spread sheet

4. Conclusion

While all three methods are generally based on the same collector model of ISO 9806, they differ with regard to the measurement boundaries, the permissible and required data basis, the calculation methods and the associated computational effort, as well as the required sensor technology (see Tab. 1). There are differences in the parameters used within the methods, interpreting and processing the ISO 9806 in different ways.

Note: Care should be taken if comparing efficiency of high-concentrating collectors with efficiency of non/low-concentrating collectors. The efficiency of high-concentrating collectors could in some cases relate to direct solar irradiance (beam irradiance) only – and non/low-concentrating collector will always relate to hemispherical irradiance (direct + diffuse irradiance).

The different methods were developed for different application purposes and therefore deliver dissimilar results with varying or selectable uncertainty levels, which are not analyzed in detail yet. Thus, they neither compete with nor contradict each other, but may even complement each other. It is therefore important for manufacturers, planners and operators of plants to first define the objectives of a measurement campaign, the expected information and accuracies as well as acceptable time and cost effort precisely before deciding on a procedure. Fig. 9 shows, in a simplified schematic way, the information provided by the methods and the requirements for which they are designed.

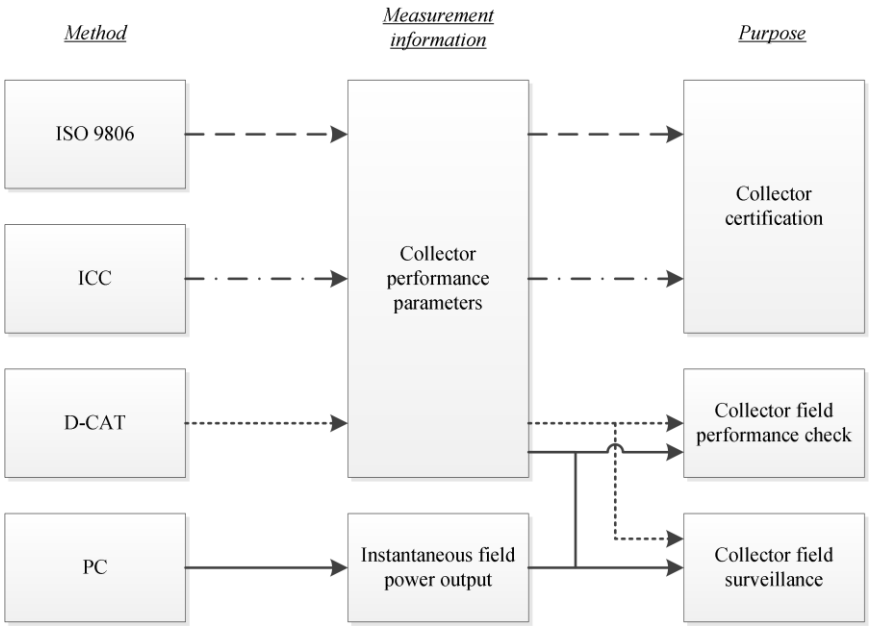

Fig. 9: Measurement purposes versus applicable methods

5. Acknowledgments

The project *ZeKon in-situ* (FK 0325560) was funded by the German Federal Ministry for Economic Affairs and Energy.

Daniel Tschopp and Philip Ohnewein were supported by the Austrian Research Promotion Agency within the project *MeQuSo* (FFG 848 766). Daniel Tschopp was supported by the Austrian Research Promotion Agency within the PhD Scholarship project *CollFieldEff*$^{+}$ (FFG 854735).

Development of the proposal for method for "Performance Check for Collector Arrays" (PC) has been supported by the IEA SHC Task 45, Task 55 and Task 57. Jan Erik Nielsen has been supported by the Danish National EUDP program for participation in these IEA SHC Tasks.

6. References

Appelbaum, J., 2018. The role of view factors in solar photovoltaic fields. Renewable and Sustainable Energy Reviews, 81, 161-171.

ESTIF, 2015. "Solar Thermal Markets in Europe. Trends and Market Statistics 2014." ESTIF, Brussels

Fedorov, V. V., 2013. Theory of optimal experiments. Elsevier.

Fahr, S.; Gumbel, U.; Zirkel-Hofer, A.; Kramer, K., 2018: In situ characterization of thermal collectors in field installations. Proceedings of EuroSun 2018, 1231-1240.

ISO 9806:2017(E): Solar energy — Solar thermal collectors — Test methods.

ISO/AWI 24194; Solar energy -- Collector fields -- Check of performance, https://www.iso.org/standard/78074.html?browse=tc

Lemos, J. M., Neves-Silva, R., & Igreja, J. M., 2014. Adaptive control of solar energy collector systems (Vol. 253). Springer.

LeVeque, R. J., 2002. Finite volume methods for hyperbolic problems (Vol. 31). Cambridge university press.

Nielsen, J.E., 2014: Guaranteed power output. IEA-SHC TECH SHEETS 45.A.3.1.

Nielsen, J.E., 2014: Guarantee of annual output. IEA-SHC TECH SHEETS 45.A.3.2.

SKN Working Group, 2019: SKN_N0444_Annex P5.5_In-Situ Collector Certification_R0.

Tschopp, D.; Ohnewein, P.; Hausner, R.; Rohringer, Ch., 2017: In-situ Testing of Large Collector Arrays – Challenges and Methodological Framework. Proceedings of SWC2017/SHC2017, 1-10.

Werner, W.; Spörk-Dür, M.; Mauthner, F., 2017: Solar Heat Worldwide – Edition 2017. Gleisdorf: AEE - Institute for Sustainable Technologies.

Weiss, W; Spörk-Dür, M., 2019: Solar Heat Worldwide - Edition 2019. Gleisdorf: AEE - Institute for Sustainable Technologies.

Zirkel-Hofer, A.; Perry, S.; Kramer, K.; Heimsath, A.; Scholl; S.; Platzer, W., 2018: Confidence interval computation method for dynamic performance evaluations of solar thermal collectors. Solar Energy 162, 585-596.

Appendix

Symbol	Description	Unit
A_G	Gross area of collector as defined in ISO 9488	m^2
a_1	Collector heat loss coefficient at $(\vartheta_{m,col} - \vartheta_a) = 0$	$W/(m^2 \cdot K)$
a_2	Temperature dependence of collector heat loss coefficient	$W/(m^2 \cdot K^2)$
a_3	Wind speed dependence of the collector heat loss coefficient	$J/(m^3 \cdot K)$
a_4	Sky temperature dependence of the collector heat loss coefficient	-
a_5	Effective thermal capacity of the collector	$J/(m^2 \cdot K)$
a_6	Wind speed dependence of the zero loss efficiency of the collector	s/m

a_7	Wind speed dependence of IR radiation exchange of the collector	$W/(m^2 \cdot K^4)$
a_8	Radiation losses of the collector	$W/(m^2 \cdot K^4)$
b_0	Heat transfer coefficient from solid part to fluid at ($\vartheta_{s,x}$ - $\vartheta_{f,x}$) = 0, based on gross collector area	$W/(m^2 \cdot K)$
b_1	Heat loss coefficient from solid part to ambient at ($\vartheta_{s,x}$ - ϑ_a) = 0, based on gross collector area	$W/(m^2 \cdot K)$
b_2	Temperature dependence of heat loss coefficient from solid part to ambient, based on gross collector area	$W/(m^2 \cdot K)$
b_5	Effective thermal capacity of solid part of the collector (not including the fluid), based on gross collector area	$J/(m^2 \cdot K)$
$c_{f\_A,\,x}$	Heat capacity of heat transfer fluid per square meter gross collector field area at position *x* in the collector field	$J/(kg \cdot K)$
$c_{f,,sec}$	Specific heat capacity of heat transfer fluid (water) at heat exchanger mean temperature	$J/(kg \cdot m^2)$
$c_{f,,x}$	Specific heat capacity of heat transfer fluid at position *x* in the collector field	$J/(kg \cdot K)$
E_L	Longwave irradiance ($\lambda > 3$ μm)	W/m^2
f_{safe}	Safety factor for Performance Check (PC) method, taking into account pipe and other heat losses, measurement uncertainties and other uncertainties	-
G_b	Direct solar irradiance on collectors	W/m^2
G_d	Diffuse solar irradiance, measured at the top of the collector	W/m^2
$G_{d,avg}$	Modelled average diffuse solar irradiance on the collectors, accounting for the obstructed sky and ground view for collectors within the array	W/m^2
G_{hem}	Hemispherical solar irradiance, measured at the top of the collector	W/m^2
$K_b(\theta)$	Incidence angle modifier for direct solar irradiance with one incidence angle (for flat plate collectors)	-
$K_b(\theta_L,\, \theta_T)$	Incidence angle modifier for direct solar irradiance with longitudinal and transversal angle	-
K_d	Incidence angle modifier for diffuse radiation	-
$\dot{m}_{pri}$	Mass flow on primary side	kg/s
n_{col}	Number of collectors in the collector array	-
$\dot{Q}_{sec}$	Thermal power supplied from heat exchanger	W
$\dot{Q}_{sec,est}$	Estimated thermal power of collector field, supplied at heat exchanger on secondary side	W
$\dot{Q}_{col}$	Useful power extracted from collector	W
s	Share of collector area with no shading of direct solar irradiance	-
t	Time	s
u	Surrounding air speed	m/s
u'	Reduced surroundings air speed (u‘ = u - 3 m/s)	m/s
$\dot{V}_{i,col}$	Volume flow for a single collector	m^3/s
$\dot{V}_{i,pri}$	Volume flow at heat exchanger inlet on primary side	m^3/s
$\dot{V}_{i,sec}$	Volume flow at heat exchanger inlet on secondary side	m^3/s
x	Axial coordinate for collector field model along the flow direction of the fluid	m
$\eta_{0,b}$	Peak collector efficiency ($\eta_{0,b}$ at $\vartheta_{m,col}$ - ϑ_a = 0 K) based on beam irradiance G_b	-
$\eta_{0,hem}$	Peak collector efficiency ($\eta_{0,hem}$ at $\vartheta_{m,col}$ - ϑ_a = 0 K) based on hemispherical irradiance G_{hem}	-
$(\tau\alpha)$	Effective transmittance-absorptance product	-
θ	Angle of incidence	degrees
θ_L	Longitudinal angle of incidence: angle between the normal to the plane of the collector and incident sunbeam projected into the longitudinal plane	degrees
θ_T	Transversal angle of incidence: angle between the normal to the plane of the collector and incident sunbeam projected into the transversal plane	degrees
ϑ_a	Ambient air temperature	°C
$\vartheta_{s,x}$	Solid part temperature at position *x* in the collector field	°C
$\vartheta_{f,\,x}$	Fluid temperature at position *x* in the collector field	°C
$\vartheta_{i,cf}$	Return (inlet) temperature of collector field, measured after the distribution pipes	°C
$\vartheta_{i,col}$	Return (inlet) temperature of a single collector	°C
$\vartheta_{i,pri}$	Heat exchanger inlet temperature, measured in primary loop at heat exchanger inlet	°C
$\vartheta_{i,sec}$	Heat exchanger inlet temperature, measured in secondary loop at heat exchanger inlet	°C
$\vartheta_{e,cf}$	Flow (outlet) temperature of collector field, measured before the distribution pipes	°C
$\vartheta_{e,col}$	Flow (outlet) temperature of a single collector	°C
$\vartheta_{e,pri}$	Heat exchanger outlet temperature, measured in primary loop at heat exchanger inlet	°C
$\vartheta_{e,sec}$	Heat exchanger outlet temperature, measured in secondary loop at heat exchanger outlet	°C
$\vartheta_{m,cf}$	Mean temperature of heat transfer fluid for collector field	°C
$\vartheta_{m,col}$	Mean temperature of heat transfer fluid for collector	°C
$\rho_{i,pri}$	Density of heat transfer fluid at heat exchanger inlet temperature on primary side	kg/m^3
$\rho_{i,sec}$	Density of heat transfer fluid (water) at heat exchanger inlet temperature on secondary side	kg/m^3
σ	Stefan-Boltzmann constant	$W/(m^2 \cdot K^4)$